Agrociencia

PHENOTYPIC DIVERSITY IN *Calendula officinalis* L. REGARDING PLANT GROWTH, PHOTOSYNTHETIC TRAITS, FLOWER YIELD, AND OIL CONTENT

Luis Francisco **Salomé-Abarca**[1], Víctor Arturo **González-Hernández**[2*], Ramón Marcos **Soto-Hernández**[3], Iván **Ramírez-Ramírez**[2], Nicacio **Cruz-Huerta**[4]

[1]Colegio de Postgraduados. Posgrado de Recursos Genéticos y Productividad-Fruticultura. Carretera México-Texcoco Km. 36.5. Montecillo, Texcoco de Mora, México. Z. C. 56264.
[2]Colegio de Postgraduados. Posgrado de Recursos Genéticos y Productividad-Genética. Carretera México-Texcoco Km. 36.5. Montecillo, Texcoco de Mora, México. Z. C. 56264.
[3]Colegio de Postgraduados. Posgrado en Botánica. Carretera México-Texcoco Km. 36.5. Montecillo, Texcoco de Mora, México. Z. C. 56264.
[4]Colegio de Postgraduados. Posgrado de Recursos Genéticos y Productividad-Fisiología Vegetal. Carretera México-Texcoco Km. 36.5. Montecillo, Texcoco de Mora, México. Z. C. 56264.
* Author for correspondence: vagh@colpos.mx

Citation: Salomé-Abarca, LF, González-Hernández VA, Soto-Hernández RM, Ramírez-Ramírez I, Cruz-Huerta N. 2024. Phenotypic diversity in *Calendula officinalis* L. regarding plant growth, photosynthetic traits, flower yield, and oil content. **Agrociencia.** https://doi.org/ 10.47163/agrociencia.v58i4.2922

Editor in Chief:
Dr. Fernando C. Gómez Merino

Received: December 11, 2022.
Approved: June 06, 2024.
Published in Agrociencia: June 24, 2024.

ABSTRACT

Pot marigold (*Calendula officinalis* L.) is an annual herb-shrub distributed worldwide. It possesses multiple therapeutic applications as an antimicrobial, antioxidant, antiviral, anti-inflammatory, anti-cancer, and cosmetic agent. Despite its importance, its physiological traits, including photosynthetic parameters, plant growth kinetics, and oil content variation among phenotypes, remain unknown. Five contrasting phenotypes (S1 to S5), derived from a single variety, were characterized. Physiological variables evaluated included plant growth kinetics, growth rate indexes, A-C_i response curves, flower and oil yield, and oil chemical composition across eight harvesting dates. Phenotype S1 yielded the highest biomass because of its extended acceleration and deceleration growth stages during a longer period. Phenotype S1 also produced higher yields of harvested flowers and essential oil. Phenotype S2 also showed a high content of essential oils. This phenotypic diversity found in a single variety of pot marigold could be used for breeding this crop; for example, the crossing of S1 x S2 may produce F1 progenies with improved growth rates, flower yields, photosynthetic rates, and essential oil yield. Besides, phenotype S1 could be used directly for commercial planting.

Keywords growth rate, growth stages, leaf area, essential oil, δ-cadinene.

INTRODUCTION

Pot marigold (*Calendula officinalis* L.) is an annual herb-shrub distributed and cultivated worldwide that stands out because of its beautiful yellow-orange colors (Givol *et al.*, 2019). This species is widely recognized for its multiple medicinal properties, which include antibacterial, antifungal, antioxidant, antiviral, anti-inflammatory, and anti-cancer effects, as well as cosmetic applications (Muley *et al.*, 2009; Jan *et al.*, 2018; Silva

et al., 2021; Jabborova *et al*., 2019; Cruceriu *et al*., 2018; Mur *et al*., 2021). These multiple benefits are linked to specialized metabolites such as essential oils, carotenoids, and flavonoids (Salomé-Abarca *et al*., 2015; Ashwlayan *et al*., 2018). Pot marigold breeding has been focused on improving four traits: ornamental value, flower yield and oil volume per hectare, medicinal-derived product quality, and plant resistance to diseases and pests. Thus, new pot marigold cultivars should grow efficiently, allocate more biomass to flowers, and produce a higher flower yield (Zitterl-Eglseer *et al*., 2001; Baciu *et al*., 2013; Samatadze *et al*., 2019). In addition, the physiological and chemical characterization of the phenotypic variation in traits like photosynthesis, growth, and metabolite content should help identify outstanding individuals.

In this context, in the Central High Valleys of Mexico, morphological and pigment variation among individual plants of a common and heterogeneous variety was reported (Soto-Hernández *et al*., 2013). Such variation also included differences in flower yields. From these variants, five phenotypes were selected based on their persistent and stable flower traits (Figure 1). This study focused on the physiological characterization of these five selected phenotypes regarding plant growth efficiency, photosynthetic parameters in response to leaf internal CO_2 concentrations, flower/oil yield, and oil chemical composition. The study determined what growth characteristics are determinants of higher total biomass accumulation and flower/oil yield and proposed the best phenotypes for pot marigold breeding and commercial production.

Figure 1. Flower heads of five selected phenotypes of pot marigold (*Calendula officinalis* L.) named from S1 to S5.

MATERIALS AND METHODS

Greenhouse and field management

Seeds from each phenotype were germinated under greenhouse conditions in trays with 200 cavities filled with a 1:1 forest soil:peat moss mixture, and each cavity received one seed. The 90-day-old seedlings were then transplanted to a field experimental station at 19° 19′ N, 98° 53′ W, at an altitude of 2250 m (29.8 °C maximum, 10.4 °C minimum, 39.6 mm of rain). Plants were distributed into 95 cm-wide rows, with 60 cm between plants along the row, achieving a planting density of 22 600 plants ha^{-1}. The

experimental unit was three rows of 5 m long. The five phenotypes were randomly assigned in a completely randomized design with three replicates. The field-grown plants were fertilized three times: twice with Bayfolan Forte™ (11.5N-8P-6K, Bayer) sprayed at 20 and 40 days after transplant (DAT), and one third time with Yaramila™ Complex (12N-11P-18K) applied at 90 DAT. Plants were irrigated every 2 weeks, except during the rainy season.

Plant growth analysis

For this analysis, one plant per phenotype and per replicate was sampled every 2 weeks for 16 weeks. Each sampled plant was dissected into leaves, stems, roots, and mature and immature flower heads (when present). All plant organs were oven-dried at 70 °C (Riosa™ Inc., Mexico) for 72 h. The dry weight of each organ, representing the accumulated biomass at each sampling date, was measured with an analytical scale (Explorer™, Ohaus, USA). The averages of organ weight (n = 3) for each phenotype and sampling date were plotted against plant age, and then several growth models were tested for each curve. The best-fit equations per organ and phenotype were chosen according to the highest coefficient of determination (R^2) provided by the software Curve Expert Professional V. 2.0™, as reported by the logistic model (Equation 1). To visually appreciate the fitness of predicted data against recorded data, both were plotted on the same graph. The growth phases for each phenotype were determined by the changes in their growth rates across the season, according to the predicted data:

$$Y = \frac{a}{(1 + be^{-cx})} \quad (1)$$

where a = asymptotic weight; b = initial weight; e = Euler's number (2.7182); c = growth rate; and x = days after transplant.

Growth rate analysis

Growth rates (GR) and relative growth rates (RGR) were calculated using the formulas quoted by Kumar *et al.* (2018) from data predicted by the best-fit models (Equations 2 and 3). Biomass allocation was assessed for two organ groups: vegetative and reproductive organs. GR (in g d^{-1}) was calculated as follows:

$$GR = (P2 - P1) / (t2 - t1) \quad (2)$$

where $P1$ and $P2$ = dry weights at two successive samplings; and $t1$ and $t2$ = days after transplant at sampling dates 1 and 2.

RGR (in g g^{-1} d^{-1}) was calculated as follows:

$$RGR = ln\ (P2 - P1) / ln\ (t2 - t1) \quad (3)$$

where *ln* = natural logarithm (based on Euler's number, 2.71828); *P*1 and *P*2 = predicted dry weights at two successive sampling dates; and *t*1 and *t*2 = days after transplant at dates 1 and 2.

The sink strength (SSt) per organ was estimated by the product of the sink size (SSz, in grams of biomass) multiplied by the sink activity (SA, estimated by the relative growth rate RGR, in g g^{-1} d^{-1}), as previously reported by Aguilar-León *et al*. (2006).

Leaf area (LA)

The leaf area per plant was measured on each fresh individual leaf separated from every-plant in each phenotype (three plants per phenotype). LA measurements were done with a leaf area meter LI-3100® (LICOR, Inc.; Lincoln, NE, USA), and means were expressed in cm^2 per plant ± standard deviation.

Flower yield

Four plants per phenotype were sampled to determine flower yield per plant at eight harvesting dates (n = 160). The initial flower sampling was done when 30 % of the plants had started to bloom; thereafter, only fully open, mature flowers were harvested every week. Flowers were harvested manually by cutting right under their bases and oven-dried at 40 °C for 48 h. The flower dry weight was measured with an analytical scale (Explorer™, Ohaus, USA), and the total flower dry weight per plant (sum of the 8 harvest dates) was reported as floral yield (g $plant^{-1}$) and as floral biomass per hectare (kg ha^{-1}) ± standard deviation (n = 4).

Photosynthetic kinetics (*A*-C_i curves)

A photosynthetic curve for each marigold phenotype was constructed with the following traits: instantaneous photosynthetic rate (*A*) at the youngest-mature leaf per plant, in response to increasing concentrations of atmospheric CO_2 (*Co*) and intracellular CO_2 (*Ci*), in four different plants per phenotype (n = 20). A portable infrared gas analyzer (LI-COR model LI-6400™, USA) was used for these measurements. This equipment was coupled to a LICOR CO_2 dispenser (LI-COR 6400-01™) to provide the following series of CO_2 concentrations for each curve: 400, 300, 200, 100, 0, 400, 600, 800, 1200, and 1600 μmol CO_2 mol^{-1}. In each replicate, the environmental conditions were kept at 21 °C for leaf temperature and 45 % relative humidity. All measurements were done under field conditions between 11:00 and 14:00 h, under completely clear skies, on randomly selected plants for each phenotype.

The LI-6400 analyzer calculated the C_i for each measured leaf based on the *Co*. The *A*-*Ci* curves for each phenotype were constructed with the averages (n = 4) of *A* and *Ci* for each CO_2-imposed concentration. A trend line was then adjusted by linear and non-linear regressions to each graph, and the compensation and saturation points (CP and SP) were estimated from the adjusted curves. The rubisco efficiency was calculated by fitting a linear regression in the transition zone between respiration

and photosynthesis. The maximum carboxylation velocity (V_{cmax}), ribulose phosphate regeneration (J_{max}), and the use of triose phosphates (TPU_{max}) were calculated with the program developed by Sharkey *et al.* (2007).

Enfleurage

Essential oils were extracted by the enfleurage technique applied to the dried inflorescences harvested from each marigold phenotype at four harvesting dates. Briefly, 100 g of vitellaria vegetable fat (*Vitellaria paradoxa*) were heated at 40 °C until a liquid state was reached, without boiling. Immediately, 3 g of dry inflorescences were added for oil extraction at 40 °C for 20 min. The vitellaria liquid fat containing the flowers was poured on top of a glass plate placed over ice for rapid solidification. Subsequently, 5 g of flowers were spread over the solidified fat layer. After 4 d of extraction, the fat was heated again and extracted with 50 mL of cold ethanol 95 %. The aromatic extracts were centrifuged at 4499.95 X*g* for 5 min and then vacuum filtered. Ethanol was then evaporated in a rotary evaporator at 30 °C, and the extracted oils were transferred to 1.5 mL glass vials under a fume hood, to allow the remaining solvent to evaporate at room temperature. The oil yield was then calculated by multiplying the oil weight by 100 and dividing the product by the inflorescence dry weight used for extraction (8 g).

Gas chromatography coupled to mass spectrometry (GC-MS)

The chemical composition of the essential oils extracted from the five phenotypes at different harvesting dates was determined by GC-MS. A Hewlett Packard HP 6890 Series® chromatograph coupled to a single quadrupole mass detector (HP 5973) was employed to perform these analyses. The GC was equipped with an HP5-MS column (30 m x 0.250 µm and 0.25 µm stationary phase thickness). Helium (99.9 % purity) was used as carrier gas at a flow rate of 1 mL min^{-1}. The oven temperature started at 40 °C and then increased at a rate of 5 °C min^{-1} until reaching 220 °C.

Compound identification was made by comparing the obtained mass spectra with those available in the NIST library V. 2014. Additionally, *n*-alkane co-injections were done to calculate the modified Kovat indexes (KI) with the van de Dool and Kratz equation (Equation 4):

$$KI = 100 * C + 100 \frac{(t'_R) \times - (t'_R)\, c}{(t'_R)\, c + 1 - (t'_R)\, c} \quad (4)$$

where C = number of carbons in the compound; $(t'_R) \times$ = corrected retention time of the compound calculated with the toluene retention time; $(t'_R)\, c + 1$ = corrected retention time of the alkane detected after the peak of the target compound; and $(t'_R)\, c$ = retention time of the alkane detected before the target compound.

Statistical analysis

For the biomass allocation analysis, we used averaged data from the sixth (87 DAT) and seventh (102 DAT) sampling dates, which corresponded to the dates with the highest biomass accumulation in all phenotypes. These data were statistically analyzed using the Tukey test for mean comparisons ($p \leq 0.05$). Flower yields were analyzed, considering phenotype and harvest date as the sources of variation in a completely randomized experimental design under a factorial arrangement of treatments (phenotype x harvest date). All tests ($p \leq 0.05$) were done with the statistical software SAS V. 8.1 (SAS Institute).

RESULTS AND DISCUSSION

Plant growth analyses

The five marigold phenotypes showed sigmoidal growth kinetics with four or five stages (La, lag; A, acceleration; Li, linear; D, deceleration; and S, stationary); only S1 did not show the linear stage (Figure 2). At 87 DAT, phenotype S1 reached its highest biomass accumulation with 228 g of dry biomass per plant, a dry weight at least 20 % heavier than the other phenotypes, which accumulated less than 200 g of biomass per plant. Phenotypic contrasts were also detected on growth parameters for the logistic model: S1 had the highest values in the initial (a) and maximum (b) weight parameters, while S2 stood out by having the highest growth rate (c) (Table 1). All chosen models showed statistically high fitness values ($R^2 > 0.98$), so they are reliable models for predicting marigold growth kinetics for plants grown in environmental conditions similar to this research.

Phenotypic differences in total biomass accumulation were mainly related to longer durations of the acceleration and deceleration stages. Phenotype S1 showed the longest acceleration and deceleration stages, 45 and 30 days, respectively (Figure 2A). Besides, S1 formed leaves for 20 days more than the other phenotypes. S2 showed a faster acceleration stage (Figure 2B), but it only lasted 32 days, and its plants grew 11 days less than S1. Conversely, S3 showed the lowest biomass accumulation rate during its short acceleration stage (Figure 2C) and ended with the lowest total biomass. Phenotypes S4 and S5 showed similar trends to those of S3 (Figures 2D and 2E). These analyses demonstrate that the acceleration and deceleration stages are the most determinant growth stages for biomass accumulation in marigold plants.

Other important phenotypic differences occurred in biomass allocation among plant organs. Flower heads, the most economically important organ in marigold, represented only 3.34 to 6.67 % of total biomass. Phenotype S1 stood out by its highest stem biomass accumulation and S2 by its higher biomass accumulation in leaves and inflorescences ($p < 0.05$). On the other hand, S5 and S3 were distinguished by allocating more biomass to roots ($p < 0.05$); phenotype S4 always showed intermediate biomass allocation values (Table 2).

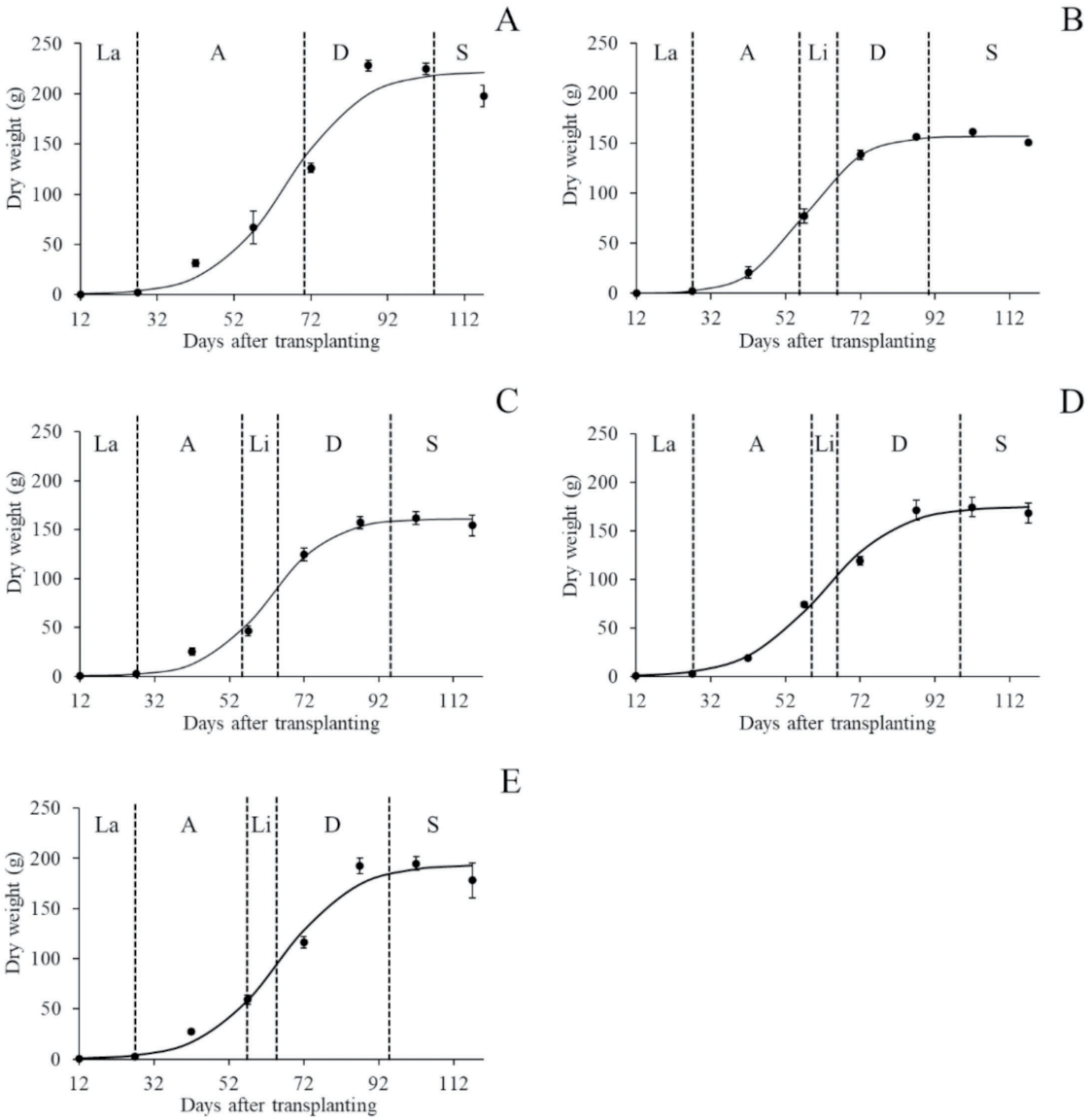

Figure 2. Growth curves of total biomass accumulation in five pot marigold (*Calendula officinalis* L.) selected phenotypes (S1 to S5), expressed in g plant^{-1}. A: phenotype S1; B: phenotype S2; C: phenotype S3; D: phenotype S4; E: phenotype S5. Growth stages L: lag; A: acceleration; Li: linear; D: deceleration; S: stationary. The data are averages of three replicates; vertical bars indicate ± standard error. The solid line represents predicted data, while solid points represent observed data.

Table 1. Values for growth parameters a, b, and c corresponding to the logistic equation $y = a/(1+be^{-cx})$ used to simulate the kinetics of total biomass accumulation in five selected phenotypes (S1 to S5) of Calendula officinalis L

Phenotype	a (g)	b	c (g g^{-1} d^{-1})	R^2
S1	2.220E+02	9.025E+02	1.033E-01	0.98
S2	1.574E+02	1.827+03	1.310E-01	0.99
S3	1.610E+02	2.014E+03	1.214E-01	0.99
S4	1.750E+02	4.467E+02	9.878E-02	0.99
S5	1.941E+02	7.187E+02	1.005E-01	0.99

a: initial weight; b: maximum weight or asymptotic weight; c: growth rate; R^2: determination coefficient per phenotype.

Table 2. Average distribution of biomass allocation among plant organs in five selected phenotypes (S1 to S5) of *Calendula officinalis* L.

Organ	S1 (g)	S2 (g)	S3 (g)	S4 (g)	S5 (g)
Stem	136.15 A	52.65 E	74.90 D	94.36 C	102.84 B
	60.12 %	33.10 %	46.97 %	54.67 %	53.10 %
Leaf	71.49 B	85.00 A	61.52 C	63.50 C	65.95 BC
	31.57 %	53.43 %	38.58 %	36.78 %	34.05 %
Root	11.24 B	10.79 B	16.82 A	7.38 C	18.08 A
	4.96 %	6.78 %	10.55 %	4.27 %	9.34 %
Flowers	7.57 B	10.64 A	6.22 C	7.38 B	6.79 BC
	3.34 %	6.69 %	3.90 %	4.27 %	3.51 %
Total	226.45 A	159.08 D	159.46 D	172.61 C	193.66 B

Values are average data (n = 6) of the sixth (87 DAT) and seventh (102 DAT) sampling dates, which correspond to the points with the highest biomass accumulation for all phenotypes. Percentage (%) of biomass assigned to each organ with respect to total biomass; S: phenotype. Phenotype mean values are compared in the same row by organs in a Tukey test ($p \leq 0.05$); different letters indicate significant differences between phenotypes.

Canopy size measured by the leaf area (LA) per plant was similar in the five phenotypes until 27 DAT; thereafter, the phenotypic differences in this trait became evident during the rest of the growing season, from 42 to 117 DAT, when S1 and S2 accumulated 14 123 and 14 601 cm^2 per plant, respectively (Figure 3). S5 only accumulated 58 % of the LA recorded in S2, with 8491 cm^2 per plant. When phenotypes S1 and S2 reached their largest LA, they already were at the stationary growth stage; their top LA (ca. 14 000 cm^2 $plant^{-1}$) was about four times higher than the one reported for marigold var. 'Bonina sortida' with 4470 cm^2 per plant (Honório *et al*., 2016). This quoted low LA

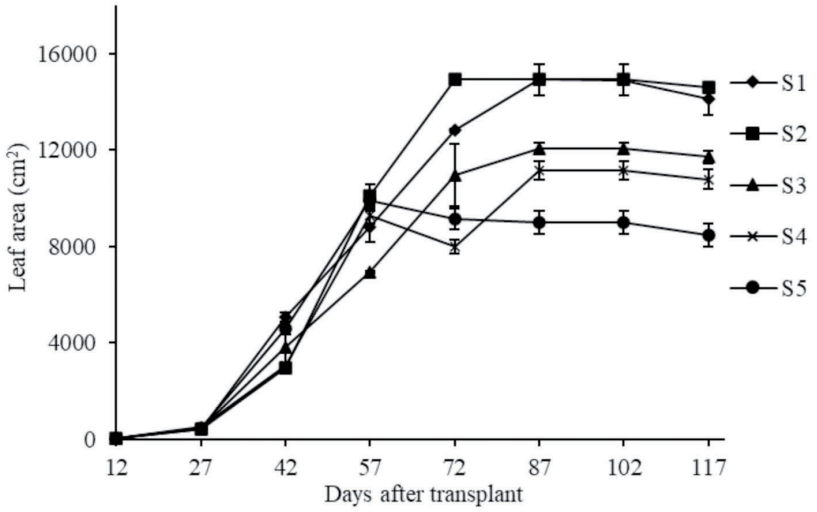

Figure 3. Kinetics of leaf area per plant in five pot marigold (*Calendula officinalis* L.) selected phenotypes (S1 to S5) measured through eight sampling dates. Data are averaged values (n = 3); vertical bars correspond to ± 1 standard deviation.

value seems to be due to the scarce flower harvestings done in that research, because it resulted in a lower branch and flower formation. Finley and Aarssen (2022) claim that periodical floral harvests in marigold promote sprouting of new shoot branches and thus a higher number of flowers.

Regarding other growth parameters of marigold, such as growth rate (GR) and relative growth rate (RGR), we found notorious contrasts among plant organs and phenotypes. For instance, the GR, which also estimates the sink strength, for the reproductive organs was about 10 times smaller than the GR for vegetative organs. This large difference between vegetative and reproductive organs may explain why calendula flowers received less than 7 % of the total biomass (Table 2). The vegetative organs reached the highest GR at 57 DAT in S2, while in the other phenotypes the peak occurred 15 days later (Figures 4A and 4B). As expected, the highest GR occurred at the end of the acceleration growth stage in all phenotypes. For the reproductive organs, the maximum GR occurred at 57 DAT in phenotypes S1, S2, S3, and S5, while in S4, the earliest phenotype, it occurred at 42 DAT. Considering all measured growth parameters, phenotypes S1 and S2 stood out for having the highest reproductive sink strength, which explains the highest biomass allocation in their flower heads (Figure 4B).

Contrary to the GR pattern, the RGR of the reproductive organs (Figures 4C and 4D) was similar to that of vegetative organs at the early stages of plant growth (up to 47 DAT). However, afterwards, the higher sink activity (i.e., higher RGR) occurred in

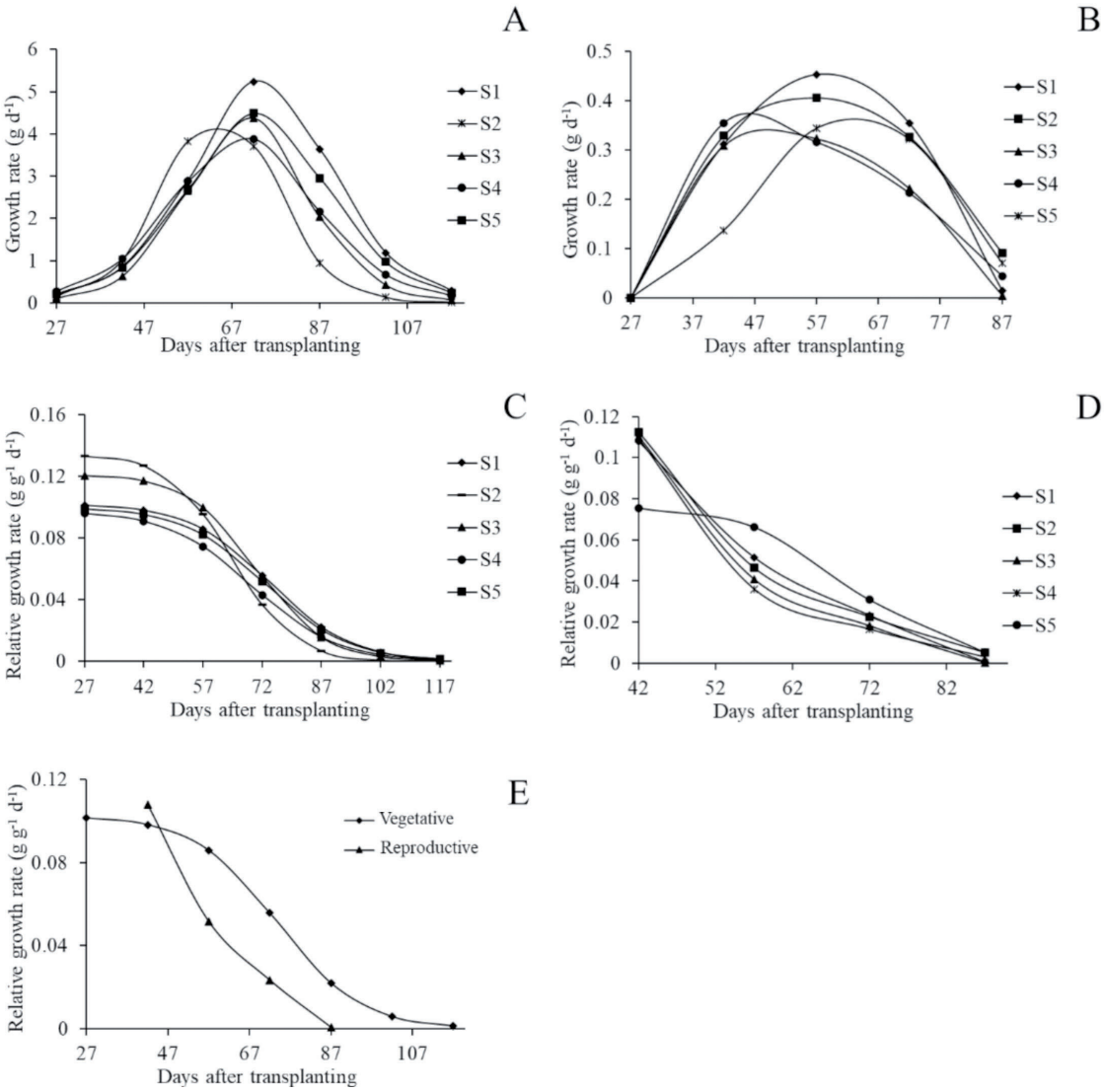

Figure 4. Growth efficiency indexes of vegetative and reproductive organs in five pot marigold (*Calendula officinalis* L.) contrasting phenotypes (S1 to S5). A: growth rates (GR) in vegetative organs; B: GR in reproductive organs; C: relative growth rates (RGR) in vegetative organs; D: RGR in reproductive organs; E: RGR of vegetative and reproductive organs in phenotype S1, which achieved the highest biomass accumulation among all phenotypes.

the vegetative organs during the rest of the growing season. This shift in sink organs may be attributed to the stem branching process, since to produce more new flower heads, new branches must be formed first. The internal competition among organs for photoassimilates clearly favors vegetative allocation, as was exemplified in phenotype S1 (Figure 4E). Moreover, at an early growth stage (42 DAT), phenotype S2 showed the highest vegetative and reproductive RGR values, 0.13 and 0.11 g g^{-1} d^{-1}, respectively. Considering that the RGR is an indicator of meristematic activity (Kumar *et al.*, 2018), then S2 is the phenotype with the most active shoot meristematic activity; in contrast, S5 had the lowest RGR value (30 % less than S2) for reproductive organs, associated with the smallest flower biomass in S5. Therefore, a high RGR value for reproductive organs might indicate a high potential to reach a higher yield. In this context, even though the RGR declines progressively as plants age, differences between phenotypes might explain the flower yield differences across harvesting dates. At the end of the growth season, the RGR phenotypic differences vanished due to a generalized decrease in the capacity to form new branches and new flowers (Figure 4D).

Photosynthetic parameters

Even though S1 was the best at biomass accumulation, this phenotype did not have the best photosynthetic features. In fact, S1 was the most limited phenotype regarding photosynthetic parameters. In general, the mathematical models obtained for the *A*/*Ci* curves of the five marigold phenotypes had good fittings between observed and predicted data (Figure 5). From these curves, it was evident that phenotype S1 has the lowest *Ci* saturation point of around 600 ppm (Figure 5A), while S2 got the highest *Ci* of c.a. 1200 ppm (Figure 5B). Phenotypes S3, S4, and S5 showed similar photosynthetic kinetics with A_{max} values in the range of 35 to 45 μmol CO_2 m^{-2} s^{-1} that occurred at *Ci* of c.a. 960 ppm (Figures 5C, D, and E).

Such photosynthetic trends allowed for the classification of the phenotypes into three groups: (1) S1 as the lowest in A_{max}; (2) S2 as the highest in A_{max}; and (3) S3, S4, and S5 with intermediate A_{max} values. The five phenotypes also showed contrasts in other photosynthetic parameters (Table 3). For instance, the CO_2 saturation point (*Psat*) needed for reaching A_{max} ranged from 30 to 74 Pa (384 to 947 ppm of *Ci*) among phenotypes, where S1 and S4, respectively, had the lowest and highest values. Therefore, S1 reached a lower *Amax* compared to the other phenotypes because of its lower ability to use high concentrations of CO_2; S1 also had the lowest rubisco efficiency among all five phenotypes (Table 3).

According to Sharkey *et al.* (2007), differences in A_{max} are associated with three limiting factors of the photosynthetic process: the maximum carboxylation rate (V_{cmax}), ribulose phosphate regeneration rate (J_{max}), and triose phosphate use (TPU_{max}). Among the five studied phenotypes, S1 had the lowest values on these three parameters (Table 4). Then, S1 may be regarded as the most limited phenotype in terms of photosynthetic potential. On the other hand, phenotypes S2 and S3 had the highest J_{max} rates; furthermore, S2 was also remarkable for its high TPU_{max}. Conversely, phenotype S3

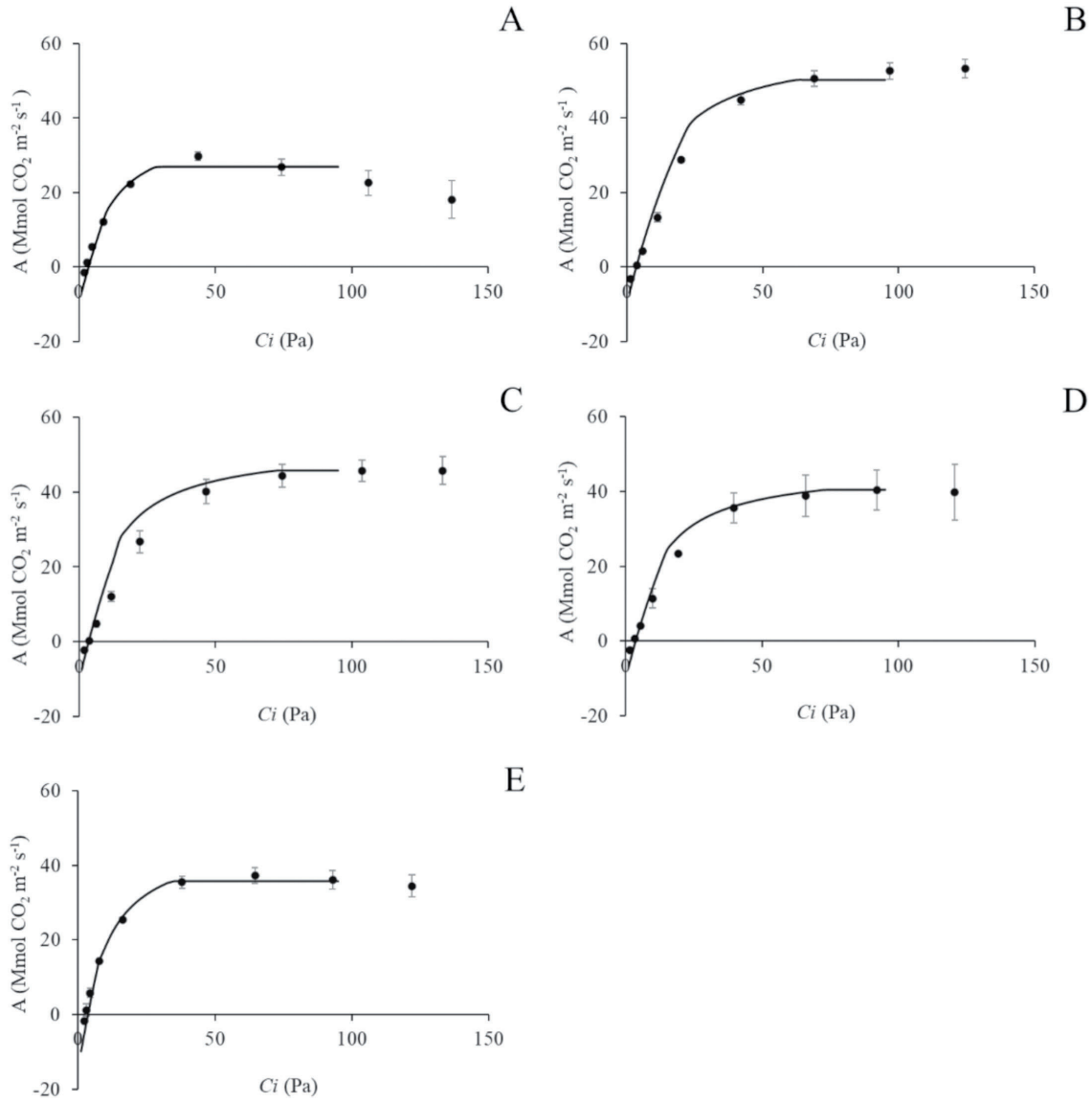

Figure 5. Kinetics of net photosynthesis rates in response to internal CO_2 concentration (*A*/*Ci* curves) of five pot marigold (*Calendula officinalis* L.) selected phenotypes (S1 to S5). A: S1; B: S2; C: S3; D: S4; E: S5. The *Ci* concentration scales are expressed in pascals (Pa); 50 Pa = 640 ppm of Ci, 100 Pa = 1280 ppm of *Ci*, and 150 Pa = 1920 ppm of *Ci*. The solid line in each graph represents predicted data by the models, while solid points represent observed data. The vertical bars on solid points represent ± standard deviation.

Table 3. Photosynthetic parameters (compensation (*PC*) and saturation (P_{sat}) points for CO_2, maximum photosynthetic rate (A_{max}), and rubisco efficiency (*REf*)) of five *Calendula officinalis* L. phenotypes (S1 to S5). The measurements were done at the blooming stage, from 77 to 84 days after transplant.

Phenotype	*PC* CO^a_2	*Psat* CO^b_2	*Amax*[c]	*Ref* [d]	SQ
S1	30.72	384	26.9	1.9	21.00
S2	42.24	793	50.1	2.0	3.02
S3	40.96	832	45.0	2.4	2.59
S4	37.12	960	40.4	2.0	7.91
S5	33.28	448	37.8	3.5	34.25

[a]expressed in ppm, [b]expressed in ppm, [c] and [d]expressed in μmol CO_2 m^{-2} s^{-1}; *SQ*: sum of squares of the model.

Table 4. Photosynthetic parameters at 25 °C calculated as proposed by Sharkey *et al.* (2007) in five selected phenotypes (S1 to S5) of pot marigold (*Calendula officinalis* L.). All measurements were done at the blooming stage, between 77 and 84 days after transplant.

Phenotype	Vc_{max}[a]	J_{max}[a]	TPU_{max}[a]	*gm*[b]
S1	127.0 ± 12.5	123.3 ± 4.6	7.6 ± 0.6	24.6 ± 0
S2	172.8 ± 7.5	279.5 ± 14.4	19.9 ± 0.9	12.6 ± 7.3
S3	204.5 ± 10.7	237 ± 14.3	17.4 ± 1.1	5.2 ± 1.5
S4	155.8 ± 12.5	211 ± 28.8	15.5 ± 2.1	24.6 ± 7.3
S5	215.8 ± 30.9	218 ± 6.9	14.8 ± 0.8	24.9 ± 9.3

Each value represents an average ± standard deviation (n = 4). V_{Cmax}: maximum carboxylation rate; J_{max}: ribulose regeneration rate; TPU_{max}: triose phosphate usage; *gm*: mesophyll conductance. [a]Data expressed in μmol m^{-2} s^{-1}, [b]data in μmol m^{-2} s^{-1} Pa^{-1}.

showed a low mesophyll conductance (*gm*), indicating a slow CO_2 diffusion into the chloroplasts, which might be a photosynthetic limitation (Evans, 2020). However, the poor condition of S3 was ameliorated by its high V_{cmax}, J_{max}, and TPU_{max} values (Table 4). Considering all the measured photosynthetic parameters, S2 may be regarded as the best phenotype for photosynthetic performance.

Compared to other plant species that have been subjected to this type of photosynthetic measurement, such as *Acacia mangium* Willd., *Buchanania arborescens* Blume, *Dillenia suffruticosa* (Griff.) Martelli, *Calophyllum inophyllum* L., and *Ploiarium alternifolium* Korth., in which the A_{max} values ranged between 10 and 13 μmol CO_2 m^{-2} s^{-1} (Benner *et al.*, 1988; Ibrahim *et al.*, 2021), our five pot marigold phenotypes showed much higher

A_{max} values (26.9 to 50.1 μmol CO_2 m^{-2} s^{-1}). The marigold A_{max} values were also higher than those of *Rubus* plant species (15 μmol CO_2 m^{-2} s^{-1}) (Mcdowell, 2002). Moreover, the V_{cmax} values of marigold phenotypes (127 to 215 μmol CO_2 m^{-2} s^{-1}) were much higher than the average V_{cmax} of herbaceous C3 plants (75 μmol m^{-2} s^{-1}) as reported by Wullschleger (1993). These comparisons indicate that pot marigold is, in general, a photosynthetically efficient species. The wide photosynthetic diversity registered in the five studied marigold phenotypes might be used for plant breeding in order to increase photosynthesis and biomass accumulation efficiency in marigold varieties. Other physiological parameters might be added to select the best progenies.

Flower and oil yield

As mentioned above, flower yield was measured only in mature open flowers, as they are commonly harvested. This means that all immature flowers were excluded for measuring flower yield, whereas for the plant growth analysis, all flowers were included, both mature and immature. According to this flower yield evaluation, S1 produced the highest flower yield among the five phenotypes (Table 5), as well as the highest biomass accumulation in the stem and in the whole plant. Since S1 also had the highest flower GR (Figure 3B), these flowers accumulated more biomass, and a larger amount of bloomed flower heads were collected at every harvest date, which explains why S1 reached the maximum flower yield among all five phenotypes.

Table 5. Flower yield of five selected phenotypes (S1 to S5) of pot marigold (*Calendula officinalis* L.) through eight harvesting dates, and the Phenotype (P) x Harvest Day (HD) interaction.

HD DAT	Phenotype S1 (kg ha^{-1})	S2 (kg ha^{-1})	S3 (kg ha^{-1})	S4 (kg ha^{-1})	S5 (kg ha^{-1})	$\bar{x}$ by HD (kg ha^{-1})
56	73.7 n…p	74.0 n…p	82.3 j…p	96.0 j…p	43.9 p	74.0 F
63	100.6 i…p	77.4 m…p	89.9 j…p	101.1 j…p	64.3 op	86.7 EF
70	127.5 h…o	80.9 l…p	97.5 i…p	106.3 i…p	84.8 j…p	99.4 E
77	264.4 a…c	217.8 b…f	232.5 b…e	173.2 e…h	185.6 d…h	214.7 B
84	235.4 b…e	236.1 b…e	237.2 b…e	179.8 d…h	184.0 d…h	214.5 B
91	309.2 a	257.0 a…c	282.2 ab	318.9 a	209.1 c…g	275.3 A
98	240.5 b…d	126.3 h…o	140.5 h…m	163.2 f…i	133.5 h…n	160.8 C
105	144.3 g…l	142.3 h…k	105.2 i…p	147.8 g…j	81.5 k…p	124.2 D
Cumulative yield per phenotype	1495.5 A	1211.9 B	1267.5 B	1286.3 B	986.7 C	
$\bar{x}$ yield by phenotype per HD	186.9 A	151.5 B	158.43 B	160.8 B	123.3 C	

Data represents the mean value across replications, expressed in kilograms of dry matter per hectare (kg ha^{-1}). Averages followed by different capital letters in a column or a row are statistically different in that column or row, according to the Tukey test ($p \leq 0.05$). Averages followed by different lowercase letters in a column or a row are statistically different in that column or row in a Tukey test ($p \leq 0.05$). DAT: days after transplant.

The second-highest flower-yielding phenotype was S2, a phenotype that also had a large leaf biomass and the lowest stem dry matter. These results suggest that the instant net photosynthesis rate (A) in all phenotypes was enough to supply sugars for plant and flower growth and for getting the highest flower yield in S1. Therefore, a high dry matter accumulation in the stem, the organ with branches where flowers are developed, is not essential to obtain a high flower yield, but stem branching is necessary for flower production, as observed in phenotype S2, which produced many flowers and obtained the second highest flower yield (Table 5). Phenotype S2 stands out for doubling the photosynthetic capacity (A_{max}) of S1.

Therefore, in marigold plants, the stem ability for branching is a trait closely associated with flower yield, and branching is promoted by periodical flower harvests. Other factors involved could be the plant architecture and leaf angle (traits not measured here), because they could modify the amount of photosynthetic active radiation (PAR) intercepted by the canopy, as pointed out by Emmel *et al.* (2020). By computing the stem biomass/leaf biomass ratio, the following morphological differences were detected between S1 and S2: S1 assigned about 60 % of total biomass to stems and 30 % to leaves (stem:leaf, 2:1), while S2 assigned around 30 % biomass to the stem and 54 % to leaves (stem:leaf, 1:2) (Table 2). This allocation comparison shows that phenotype S1 grows more branches per plant but with fewer leaves per branch, while S2 forms fewer branches but each branch has more leaves, which would probably cause differences in the intercepted PAR by each phenotype.

In pot marigold, the most valuable organs are the flowers because of their medicinal and industrial applications (Khalid and da Silva, 2012). Regarding the flower yield monitored through eight harvests across the season, there were statistical differences among phenotypes (P) and harvest dates (HD), as well as for the P x HD interaction ($p \leq 0.01$). These results clearly show that the five marigold phenotypes vary in flower yields through the cutting dates. S1 reached the highest mature flower yield accumulated through the growing season ($p < 0.05$). Interestingly, S2 allocated more biomass to flowers, including both mature and immature buds, thus possessing a higher sink strength (Table 2), a trait that could potentially be used to increase its flower yield. This phenotypic difference may be explained because S1 developed more mature flowers at each harvesting date, so with each harvest (i.e., pruning), the stem would be induced to develop a higher number of new lateral branches. On the contrary, S2 with a smaller number of mature flowers at each harvest date would induce a smaller stimulus for branching formation and, consequently, a lesser flower yield than S1.

Nonetheless, phenotype S2 has the physiological potential to reach the highest flower yield by accelerating flower development (faster maturation). Since continuous flower production across the growing season in marigold plants is prevented by apical dominance, which suppresses the development of lateral buds (required for branching). Therefore, when flowers are harvested, the apical dominance of that branch is temporarily suppressed, thus allowing the sprouting of axillary meristems for producing new branches (Finley and Aarssen, 2022). This means that each flower

harvest will promote the formation of new flowers. In marigold plants, each flower harvest also delays the leaf senescence process while promoting new secondary shoots (branches), so that periodical flower harvestings would result in a higher flower yield accumulated through the season. In pot marigold grown at Samsum, Turkey, on 24 harvesting dates over four months, the total flower yield was 566 kg ha^{-1} DW (Caliskan and Kurt, 2018), while in our study, the phenotype S1 yielded 1495 kg ha^{-1} DW in a harvesting period of only two months. Therefore, for pot marigold, the number of harvested flowers is more correlated to the flower yield than to the number of harvesting dates across the season.

Across the harvest dates, the sixth one (91 DAT) rendered the maximum flower production ($p < 0.05$). On this harvest, phenotypes S1 and S4 showed their highest yields, which are higher than those reported by Acosta-de la Luz *et al*. (2001) for pot marigold grown in Cuba (200 to 300 kg ha^{-1} DW). Considering the total flower production accumulated across the season, phenotype S1 outstands as the best in flower yield ($p < 0.05$). Interestingly, the phenotype ranking for flower yield (Table 5) matches the phenotype ranking for leaf area (Figure 2). This close association between leaf area and flower yield shows the importance of leaf surface as an important component of the source strength for suppling sugars and nutrients required for flower development and growth, considering flower yield as the most important sink strength in marigold in terms of sink-source relationships.

Essential oil content and chemical variation

The content of relevant compounds in the marigold flowers, such as carotenoids, flavonoids, and essential oils, is important because these flowers are used for medicinal and industrial purposes (Kurzawa *et al.*, 2022). The essential oils had received broad attention because of their diverse biological effects (Zengin *et al.*, 2021). In our study, phenotypes S1, S2, and S5 maintained constant oil content through the growing season, while S3 and S4 showed a notorious increment in oil yield from the first to the sixth harvest (Table 6). According to flower mass essential oil yield, phenotype S2 showed the highest oil yield. However, when combining the average floral yields (kg DW ha^{-1}) with their corresponding oil yields (g 100 g^{-1} DW) in each phenotype, the resulting oil yields for phenotypes S1, S2, S3, S4, and S5 were 6.73, 6.51, 6.18, 5.79, and 4.56 kg of oil per hectare (Table 6), respectively. In this rank, phenotypes S1, S2, and S3 stand as the best ones for oil production under the tested field conditions. S2 flowers possessed a higher content of oil, but S1 produced more flowers, thus yielding a higher amount of oil per hectare.

Regarding the types of essential oils, the chromatographic analyses showed important chemical variations among marigold phenotypes and harvesting dates. Phenotype S4 was the most diverse, with 26 identifiable volatile compounds. The metabolite diversity decreased in the other phenotypes as follows: S2 > S3 > S1 > S5, with 24, 23, 19, and 18 identified compounds, respectively (Table 7). The chemical composition of essential oils included aldehydes, monoterpenes, and sesquiterpenes. Only the

Table 6. Oil yield (relative content, %) in flowers of five selected phenotypes (S1 to S5) of pot marigold (*Calendula officinalis* L.) harvested through four dates and extracted by enfleurage.

	Phenotype					
DAT[a]	S1	S2	S3	S4	S5	$\bar{x}$ by harvest
56	3.5 ± 0.7	4.7 ± 1.4	3.7 ± 0.1	3.2 ± 0.06	3.5 ± 0.2	3.7 ± 0.52
70	3.8 ± 0.9	3.8 ± 0.4	3.3 ± 0.3	3.7 ± 0.2	3.9 ± 0.4	3.7 ± 0.21
84	3.7 ± 0.3	3.7 ± 0.3	4.0 ± 0.04	3.3 ± 0.7	3.7 ± 0.7	3.7 ± 0.22
91	3.6 ± 0.1	5.0 ± 0.1	4.6 ± 0.3	4.3 ± 0.6	3.7 ± 0.2	4.2 ± 0.53
$\bar{x}$ by phenotype	3.6 ± 0.1	4.3 ± 0.6	3.9 ± 0.5	3.6 ± 0.5	3.7 ± 0.2	

The data represent average values (n =3) ± standard deviation. [a]DAT, days after transplant.

sesquiterpenes copaene and δ-cadinene, was detected in all the phenotypes and harvesting dates (Table 7). S2 and S3 stand out as the phenotypes with the highest contents of δ-cadinene (30 to 45 % of the total oil content). This sesquiterpene has been reported as having antibacterial activity against *Streptococcus pneumoniae* (Pérez-López *et al*., 2011). According to Babahmad *et al.* (2018), essential oils with high content of cadinenes have been reported with a strong antimicrobial activity.

The chemical variation in essential oils through different harvesting dates has also been observed by other researchers (Okoh *et al*., 2007). Most compounds found here in phenotypes S1–S5 (Table 7) have been previously reported in the essential oils of pot marigold (Okoh *et al*., 2007; Gazim, 2008; Okoh *et al*., 2008; Muley *et al*., 2009; Król, 2012; Ourabia *et al*., 2019; Sahingil, 2019). In general, δ-cadinene was the most abundant volatile in all oils. This monoterpene has been previously reported in pot marigold grown in Brazil, representing 27 % of its essential oils (Gazim, 2008), which is about half the percentage found here in phenotype S3.

Moreover, three cadinene-like compounds (α-cadinene, 7-epi-α-cadinene, and α-cadinol) are also contained in our marigold oils at good percentages (Table 7). In S2, α-cadinene was present up to 7.5 % of the total oil content at the third and fifth harvesting dates. This compound has been reported to be as high as 13 % in pot marigolds (Okoh *et al*., 2008). The isomer 7-epi-α-cadinene was produced by phenotypes S2, S3, S4, and S5 on different harvesting dates, with percentages ranging from 5.5 to 7.5 %. According to Muley *et al.* (2009), this metabolite is a component of the marigold essential oil. In S5, α-cadinol reached almost 8 % of the oil composition extracted from the first harvesting date. This last metabolite is produced by other species such as *Syzygium aromatic* L. and *Juniperus communis* L. (Zheljazkov *et al*., 2017; Ayub *et al*., 2023), and it has been reported as an antifungal agent (Ho, 2011). Moreover, α-cadinol has been proposed as a cure for antibiotic-resistant tuberculosis (Bueno *et al*., 2011).

Table 7. Chemical composition of essential oils extracted from five pot marigold (*Calendula officinalis* L.) phenotypes through four harvesting dates, expressed in relative composition (%) compared to total content.

		Phenotype					Phenotype					Phenotype					Phenotype				
	KI*	S1	S2	S3	S4	S5	S1	S2	S3	S4	S5	S1	S2	S3	S4	S5	S1	S2	S3	S4	S5
		56 DAT					70 DAT					84 DAT					98 DAT				
Benzaldehyde	707	0.5	-	-	0.9	-	0.3	-	0.2	1	-	-	-	0.2	0.7	-	-	-	0.2	0.5	-
Octanal	801	-	-	-	-	-	-	-	-	1.1	-	-	-	-	-	-	-	-	-	-	-
Nonanal	1000	0.2	-	0.2	1.5	3.7	0.3	0.7	0.4	1.1	-	0.2	-	0.3	1	-	0.2	-	0.3	0.7	-
Carene	1048	0.6	-	-	-	-	-	-	-	-	-	-	-	-	-	-	-	-	-	-	-
γ-muurolene	1502	1.2	3	-	-	3.3	0.7	-	-	-	-	0.7	2.6	-	1.1	-	-	5	0.7	-	-
7-*epi*-α-cadinene	1507	-	-	1	2.9	-	-	7	2.8	7.4	6.3	-	7	2.9	5.1	4.8	-	-	0.9	6	5.5
Epizonarene	1507	-	7.5	-	-	-	-	-	-	0.2	-	-	8	-	0.2	-	-	-	-	0.2	-
Germacrene D	1510	-	-	0.2	-	-	-	-	0.2	0.9	-	-	1.5	0.1	0.5	-	-	-	0.1	-	-
Isoledene	1514	-	5.4	-	-	6.1	-	-	-	0.3	-	-	5.2	-	0.2	-	-	-	-	2.5	8.4
Viridiflorol	1514	-	-	-	-	-	-	3.1	-	-	-	-	-	-	-	-	-	-	-	-	-
α-muurolene	1515	-	-	0.5	-	-	-	-	1.3	3.7	8.4	-	1.5	-	-	7.3	-	-	-	-	-
Caryophyllene	1516	0.1	-	0.1	-	-	-	-	-	-	-	0.1	-	-	-	-	0.1	-	-	-	-
δ-cadinene	1519	5.6	29.3	2.4	3.7	32.9	6.8	41	4.7	8.2	45.8	4.5	39.9	3.9	8.4	40.8	2.4	39	1.7	7.2	44.9
α-cubebene	1520	0.4	-	0.2	-	0.7	0.7	3.7	0.4	0.5	2.9	0.4	1.7	0.2	-	1.8	0.2	2.3	0.2	-	2.4
α-cadinene	1528	2	-	-	-	-	2.4	7.6	1.1	2.4	-	1.3	-	1.2	-	-	-	7.1	-	-	-
Copaene	1533	0.6	2.2	0.3	0.5	2	0.8	3.6	0.6	0.9	3	0.6	2	0.5	1.3	2.8	0.3	2.1	0.3	0.6	3.1
Aromadendrene[b]	1547	-	-	-	0.8	-	-	-	-	-	-	-	1.8	-	0.1	-	-	-	-	0.3	1.3
β-cubebene	1550	0.7	3.7	0.3	-	2.4	1.2	5.9	0.8	0.5	5.8	0.1	3.4	0.5	-	4.7	0.3	4.1	0.3	-	5
Phellandrene[a]	1551	1.1	-	-	-	-	0.9	-	-	-	-	1	-	0.3	-	-	-	-	-	-	-
β-gurjenene	1555	0.4	-	-	-	-	-	-	-	-	-	-	-	-	-	-	-	-	-	-	-
Calarene	1556	-	-	-	-	-	-	-	-	-	-	-	-	-	0.3	-	-	-	-	0.4	-
Longifolene	1558	-	-	-	-	-	-	1.6	-	-	-	-	-	-	0.1	-	-	-	-	0.2	-
γ-gurjenene	1559	-	1.4	-	0.7	1.1	-	-	-	-	-	0.3	-	0.1	2.6	0.6	-	-	-	-	-
τ-cadinol	1560	-	-	0.2	-	6.1	-	-	0.4	-	3	0.6	3.8	0.3	-	-	0.2	-	0.1	-	3.1
τ-mururolol	1561	-	-	-	-	-	-	-	-	-	-	-	-	0.7	-	-	-	-	-	-	-
β-patchoulene	1562	-	-	-	-	-	-	-	0.1	-	-	-	-	-	-	-	-	-	-	-	-
Aromadendrene	1563	-	0.3	0.1	-	-	-	-	-	-	-	-	-	0.1	-	-	-	-	-	-	-
Valencene	1563	-	-	-	0.5	-	0.9	-	0.1	0.3	0.8	-	-	0.1	0.8	-	-	-	-	0.2	-
α-cadinol	1564	0.9	-	-	-	7.8	0.9	-	0.5	-	-	0.8	4.3	-	-	-	-	-	-	-	-
Viridiflorene	1567	-	-	-	6	-	-	-	1	-	-	-	-	-	-	-	-	-	-	3.6	-
Cedrene	1578	-	-	-	-	-	-	-	-	-	-	0.2	-	-	-	-	-	-	-	-	-
Sesquirofuran	1578	-		-	-	-	-	-	-	-	-	-	0.7	-	-	-	-	-	-	-	-
α-elemene	1584	-	-	-	-	-	-	-	-	0.2	2.6	-	1.2	-	5.2	-	-	-	-	-	-
γ-selinene	1600	-	-	-	-	-	-	-	-	0.2	-	-	-	-	-	-	-	-	-	-	4.8
α-eremofilene	1612	-	-	-	1.8	-	-	-	0.3	-	-	-	-	-	0.1	-	-	-	-	-	-

*Retention index; [a]epi-bicyclosesquiphellandrene; [b]alloaromadendrene; [c]DAT: days after transplant.

CONCLUSIONS

Five phenotypes derived from a single common variety of pot marigold showed large contrasts in plant growth, photosynthetic parameters, flower yield, essential oil content, and metabolite composition through eight harvesting dates. Phenotypic differences in total biomass accumulation were positively associated with the duration of the acceleration and deceleration growth phases. That is, longer acceleration and deceleration phases provided higher total biomass accumulation. Phenotype S1 stands out as the most efficient for total biomass accumulation, flower yield, and essential oils yield. Regarding growth parameters, high growth rates (GR) serve as a selection parameter for high biomass accumulation phenotypes. On the other hand, high relative growth rate (RGR) values in vegetative organs might serve as a selection criterion for obtaining phenotypes that would produce more branches where flowers are generated, while selecting phenotypes with higher GR in reproductive organs would lead to select marigold plants able to allocate more biomass to individual flowers (bigger flowers).

The marigold phenotypic differences in photosynthetic potential are mainly determined by high values of max rates of carboxylation (V_{cmax}), ribulose regeneration (J_{max}), and triose phosphate usage (TPU_{max}) S2 stood out as the most efficiente phenotype in several photosynthesis parameters, contrasting with S1, which was the least efficient in this process. The apparent contradiction of phenotype S1 possessing the highest total biomass accumulation and flower yield while having the worst photosynthetic parameters could be explained by a larger total leaf area, a high branching rate, and a convenient branch/leaf architecture. Therefore, physiological parameters are useful traits for selecting efficient pot marigold varieties. Phenotypes S1 and S2 are the best candidates for breeding programs as they combine several important physiological traits, such as net photosynthetic rate, growth rate, and flower and oil yields.

ACKNOWLEDGEMENTS

To the *Colegio de Postgraduados* (Mexico) for financing all the research expenses, and to CONACYT-Mexico for providing a M. Sc. Scholarship to the first author.

REFERENCES

Acosta-de la Luz L, Rodríguez-Ferradá C, Sánchez-Govín E. 2001. Instructivo técnico de *Calendula officinalis*. Revista Cubana de Plantas Medicinales 6 (1): 23–27.

Aguilar-León MG, Carrillo-Salazar JA, Rivera-Peña A, González-Hernández VA. 2006. Análisis de crecimiento y de relaciones fuente-demanda en dos variedades de papa (*Solanum tuberosum* L.). Revista Fitotecnia Mexicana 29 (2): 145–156. https://doi.org/10.35196/rfm.2006.2.145

Ashwlayan VD, Kumar A, Verma M, V Kumar, Garg SK, Gupta M. 2018. Therapeutic potential of *Calendula officinalis*. Pharmacy and Pharmacology International Journal 6 (2): 149–155. https://doi.org/10.15406/ppij.2018.06.00171

Ayub MA, Goksen G, Fatima A, Zubair M, Abid MA, Starowicz M. 2023. Comparison of conventional extraction techniques with superheated steam distillation on chemical characterization and biological activities of *Syzygium aromaticum* L. essential oil. Separations 10 (1): 27. https://doi.org/10.3390/separations10010027

Babahmad RA, Aghraz A, Boutafda A, Papazoglou EG, Tarantilis PA, Kanakis C, Hafidis M, Ouhdouch Y, Outzourhit A, Ouhammou A. 2018. Chemical composition of essential oil of *Jatropha curcas* L. leaves and its antioxidant and antimicrobial activities. Industrial crops and products 121: 405–410. https://doi.org/10.1016/j.indcrop.2018.05.030

Baciu AD, Pamfil D, Mihalte L, Sestras AF, Sestras RE. 2013. Phenotypic variation and genetic diversity of *Calendula officinalis* (L). Bulgarian Journal of Agricultural Science 19 (1): 143–151.

Benner P, Sabel P, Wild A. 1988. Photosynthesis and transpiration of healthy and diseased spruce trees in the course of three vegetation periods. Trees 2 (4): 223–232. https://doi.org/10.1007/bf00202377

Bueno J, Escobar P, Martínez JR, Leal SM, Stashenko EE. 2011. Composition of three essential oils, and their mammalian cell toxicity and antimycobacterial activity against drug resistant-tuberculosis and nontuberculous mycobacteria strains. Natural Product Communications 6 (11): 1743–1748. https://doi.org/10.1177/1934578x1100601143

Caliskan O, Kurt D. 2018. Flower yields of pot marigold (*Calendula officinalis* L.) plants as effected by flowering durations and number of harvests. Journal of Medicinal Plants Studies 6 (6): 159–161.

Cruceriu D, Balacescu O, Rakosy E. 2018. *Calendula officinalis*: potential roles in cancer treatment and palliative care. Integrative Cancer Therapies 17 (4): 1068–1078. https://doi.org/10.1177/1534735418803766

Emmel C, D'Odorico P, Revill A, Hörtnagl L, Ammann C, Buchmann N, Eugster W. 2020. Canopy photosynthesis of six major arable crops is enhanced under diffuse light due to canopy architecture. Global Change Biology 26 (9): 5164–5177. https://doi.org/10.1111/gcb.15226

Evans JR. 2021. Mesophyll conductance: walls, membranes and spatial complexity. New Phtologist 229 (4): 1864–1876. https://doi.org/10.1111/nph.16968

Finley JV, Aarssen LW. 2022. No evidence of a generalized potential 'cost' of apical dominance for species that have strong apical dominance. Journal of Plant Ecology 15 (6): 1168–1184. https://doi.org/10.1093/jpe/rtac053

Gazim ZC, Rezende CM, Fraga SR, Filho BPD, Nakamura CV, Cortez DAG. 2008. Analysis of the essential oils from *Calendula officinalis* growing in Brazil using three different extraction procedures. Brazilian Journal of Pharmaceutical Sciences 44 (3): 391–395. https://doi.org/10.1590/s1516-93322008000300008

Givol O, Kornhaber R. Visentin D, Cleary M, Haik J, Harats M. 2019. A systematic review of *Calendula officinalis* extract for wound healing. Wound Repair and Regeneration 27 (5): 548–561. https://doi.org/10.1111/wrr.12737

Ho CL, Liao PC, Wang EIC, Su YC. 2011. Composition and antifungal activities of the leaf essential oil of *Neolitsea parvigemma* from Taiwan. Natural Product Communications 6 (9): 1357–1360. https://doi.org/10.1177/1934578x1100600935

Honório ICG, Bonfim FPG, Montoya SG, Casali VWD, Leite JPV, Cecon PR. 2016. Growth, development and content of flavonoids in calendula (*Calendula officinalis* L). Acta Scentiarum Agronomy 38 (1): 69–75. https://doi.org/10.4025/actasciagron.v38i1.25976

Ibrahim MH, Sukri RS, Tennakoon KU, Le QV, Metali, F. 2021. Photosynthetic responses of invasive *Acacia mangium* and coexisting native heath forest species to elevated temperature and CO_2 concentrations. Journal of Sustainable Forestry 40 (6): 573–593. https://doi.org/10.1080/10549811.2020.1792317

Jabborova D, Davranov K, Egamberdieva D. 2019. Antibacterial, antifungal, and antiviral properties of medical plants. *In* Egamberdieva D, Tiezzi A. (eds.), Microorganisms for Sustainability. Springer: Singapore, pp: 51–65. https://doi.org/10.1007/978-981-13-9566-6_3

Jan N, Majeed U, Andrabi KI, John R. 2018. Cold stress modulates osmolytes and antioxidant system in *Calendula officinalis*. Acta Physiologiae Plantarum 40 (4): 1–16. https://doi.org/10.1007/s11738-018-2649-0

Khalid KA, da Silva JT. 2012. Biology of *Calendula officinalis* Linn.: focus on pharmacology, biological activities and agronomic practices. Medicinal and Aromatic Plant Science and Biotechnology 6 (1): 12–27.

Król B. 2012. Yield and chemical composition of flower heads of selected cultivars of pot marigold (*Calendula officinalis* L). Acta Scientiarum Polonorum Hortorum Cultus 11 (1): 215–225.

Kumar V, Singh J, Chopra AK. 2018. Assessment of plant growth attributes, bioaccumulation, enrichment, and translocation of heavy metals in water lettuce (*Pistia stratiotes* L.) grown in sugar mill effluent. International Journal of Phytoremediation 20 (5): 507–521. https://doi.org/10.1080/ 15226514.2017.1393391

Kurzawa M, Wilczyńska E, Brudzyńska P, Sionkowska A. 2022. Total phenolic content, antioxidant capacity and UV radiation protection properties of marigold (*Calendula officinalis*), carrot (*Daucus carota*), tomato (*Solanum lycopersicum*) and hop (*Humulus lupulus*) Extracts. Cosmetics 9 (6): 134. https://doi.org/10.3390/cosmetics9060134

McDowell SCL. 2002. Photosynthetic characteristic of invasive and non-invasive species of *Rubus* (Rosaceae). American Journal of Botany 89 (9): 1431–1438. https://doi.org/10.3732/ajb.89.9.1431

Muley BP, Khadabadi SS, Banarase NB. 2009. Phytochemical constituents and pharmacological activities of *Calendula officinalis* Linn (Asteraceae): A review. Tropical Journal of Pharmaceutical Research 8 (5): 455–465. https://doi.org/10.4314/tjpr.v8i5.48090

Mur R, Langa E, Pino-Otín MR, Urieta JS, Mainar AM. 2021. Concentration of antioxidant compounds from *Calendula officinalis* through sustainable supercritical technologies, and computational study of their permeability in skin for cosmetic use. Antioxidants 11 (1): 96. https://doi.org/10.3390/antiox11010096

Okoh OO, Sadimenko AP, Asekun OT, Afolayan AJ. 2008. The effects of drying on the chemical components of essential oils of *Calendula officinalis* L. African Journal of Biotechnology 7 (10): 1500–1502.

Okoh OO, Sadimenko AP, Afolayan AJ. 2007. The effects of age on the yield and composition of the essential oils of *Calendula officinalis*. Journal of Applied Sciences 7 (23): 3806–3810. https://doi.org/10.3923/jas.2007.3806.3810

Ourabia I, Djebbar R, Tata S, Sabaou N, Fouial-Djebbar D. 2019. Determination of essential oil composition, phenolic content, and antioxidant, antibacterial and antifungal activities of marigold (*Calendula officinalis* L.) cultivated in Algeria. Carpathian Journal of Food Science and Technology 11 (2): 93–110. https://doi.org/10.34302/crpjfst/2019.11.2.8

Pérez-López A, Cirio AT, Rivas-Galindo VM, Aranda RS, de Torres NW. 2011. Activity against *Streptococcus pneumoniae* of the essential oil and δ-cadinene isolated from *Schinus molle* fruit. Journal of Essential Oil Research 23(5): 25–28. DOI: 10.1080/10412905.2011.9700477

Sahingil D. 2019. GC/MS-olfactometric characterization of the volatile compounds, determination antimicrobial and antioxidant activity of essential oil from flowers of calendula (*Calendula officinalis* L.). Journal of Essential Oil Bearing Plants 22 (6): 1571–1580. https://doi.org/10.1080/0972060x.2019.1703829

Salomé-Abarca LF, Soto-Hernández RM, Cruz-Huerta N, González-Hernández VA. 2015. Chemical composition of scented extracts obtained from *Calendula officinalis* by three extraction methods. Botanical Sciences 93 (3): 633–638. https://doi.org/10.17129/botsci.143

Samatadze TE, Zoshchuk SA, Hazieva FM, Yurkevich OY, Svistunova NY, Morozov AI, Amosova AV, Muravenk OV. 2019. Phenotypic and molecular cytogenetic variability in calendula (*Calendula officinalis* L) cultivars and mutant lines obtained via chemical mutagenesis. Scientific Reports 9 (1): 9155. https://doi.org/10.1038/s41598-019-45738-3

Sharkey TD, Bernacchi CJ, Farquhar GD, Singsaas EL. 2007. Fitting photosynthetic carbon dioxide response curves for C3 leaves. Plant, Cell and Environment 30 (9): 1035–1040. https://doi.org/10.1111/j.1365-3040.2007.01710.x

Silva D, Ferreira MS, Sousa-Lobo JM, Cruz MT, Almeida IF. 2021. Anti-Inflammatory activity of *Calendula officinalis* L. flower extract. Cosmetics 8 (2): 31. https://doi.org/10.3390/cosmetics8020031

Soto-Hernández RM, Palma-Tenango M, González-Hernández VA. 2013. Carotenoid content in six genotypes of *Calendula officinalis* L. through harvesting dates in Mexico. Planta Medica 79 (10): PS8. https://doi.org/10.1055/s-0033-1348822

Wullschleger SD. 1993. Biochemical limitations to carbon assimilation in C3 plants-A retrospective analysis of the A/Ci curves from 109 Species. Journal of Experimental Botany 44 (5): 907–920. https://doi.org/10.1093/jxb/44.5.907

Zengin G, Mahomoodally MF, Sinan KI, Sadeer N, Maggi F, Caprioli G, Angeloni S, Mollica A, Stefanucci A, Ak G, Cakılcıoglu U, Polat R., Akan H. 2021. Evaluation of chemical constituents and biological properties of two endemic *Verbascum* species. Process Biochemistry 108: 110–120. https://doi.org/10.1016/j.procbio.2021.06.007

Zheljazkov VD, Astatkie T, Jeliazkova EA, Heidel B, Ciampa L. 2017. Essential oil content, composition and bioactivity of Juniper species in Wyoming, United States. Natural Product Communications 12 (2): 201–204.

Zitterl-Eglseer K, Reznicek G, Jurenitsch J, Novak J, Zitterl W, Franz C. 2001. Morphogenetic variability of faradiol monoesters in marigold *Calendula officinalis* L. Phytochemical Analysis 12 (3): 199–201. https://doi.org/10.1002/pca.582.